Evidence for pre-processing and dynamical evolution for low-mass satellite galaxies

Ian D. Roberts,⋆ Laura C. Parker
Department of Physics and Astronomy, McMaster University, Hamilton ON L8S 4M1, Canada

ABSTRACT
We study the dependence of satellite star formation rate and morphology on group dynamics for a sample of SDSS groups. We classify the group dynamics and study satellite properties for populations of virialized and infalling galaxies. For infalling galaxies we find no differences in the star-forming or disc fraction for those infalling onto Gaussian groups compared to those infalling onto non-Gaussian groups. By comparing the star-forming and disc fractions of infalling galaxies to field galaxies we find evidence for the pre-processing of both star formation rate and morphology. The strength of pre-processing shows a clear increase with halo mass and is highest for low-mass galaxies infalling onto high-mass haloes. When considering galaxies within the virialized region of the halo we show that a dependence on group dynamical state emerges, with low-mass galaxies in non-Gaussian groups showing enhanced star-forming and disc fractions compared to galaxies in Gaussian groups. This suggests that either the mechanisms driving star formation quenching and morphological transformations within the virial radius are more efficient in dynamically relaxed groups, or that non-Gaussian groups have assembled more recently and therefore satellites of the groups will have been exposed to these transforming mechansims for less time.

Key words: galaxies: clusters: general – galaxies: evolution – galaxies: groups: – galaxies: statistics

1 INTRODUCTION

In the first half of the twentieth century it was beginning to be realized that populations of high-mass clusters were predominantly made up of early-type galaxies, with Hubble & Humason (1931) stating that, "The predominance of early types is a conspicuous feature of clusters in general". Many subsequent observational studies have cemented the now familiar environmental dependence of galaxy properties (e.g. Butcher & Oemler 1978; Dressler 1980; Postman & Geller 1984; Dressler et al. 1999; Blanton et al. 2005; Wetzel et al. 2012). Namely, galaxies in galaxy clusters, tend to be red in colour with low star formation rates and early-type morphologies. On the other hand the low-density field is preferentially populated by blue, star forming, spiral galaxies. A third environment, galaxy groups, are the most common environment in the local Universe (Geller & Huchra 1983; Eke et al. 2005) and also represent an intermediate-mass regime in which significant populations of both star-forming spirals and passive ellipticals are observed (e.g. Wilman et al. 2005; McGee et al. 2011).

Not only do galaxy properties correlate with the type of haloes in which they reside, but also with radial distance from the halo centre. In particular, galaxies at large radii show enhanced star formation and are more likely to have spiral morphologies compared to galaxies near the centre of halo (Whitmore et al. 1993; Goto et al. 2003; Postman et al. 2005; Rasmussen et al. 2012; Wetzel et al. 2012; Fasano et al. 2015; Haines et al. 2015). Therefore in order to probe the environmentally driven aspects of galaxy evolution it is crucial to account for both the dependence on the host halo environment as well as the radial position within the group or cluster. Furthermore, one can consider the position of galaxies in velocity-radius phase space to divide galaxies into three main classes: those infalling onto the cluster, those within the virialized region, and those "backsplashing" out to large radii after a passage through the halo centre (e.g. Mahajan et al. 2011). Galaxies in these different regions can have distinct properties, for instance backsplash galaxies should have lower masses due to tidal mass loss (Gill et al. 2005), infalling galaxies have been shown to have enhanced specific star formation rates (Noble et al. 2016), and post-starburst galaxies seem to occupy intermediate regions in phase-space (Muzzin et al. 2014).

The aforementioned environmental dependences are strongest for low-mass galaxies and it appears that prop-

erties of high-mass galaxies are less dependent on environment (Haines et al. 2006; Bamford et al. 2009). For high-mass galaxies quenching is thought to be driven by internal, secular processes such as feedback from AGN (e.g. Schawinski et al. 2009). This dichotomy between high and low mass galaxies is presented in Peng et al. (2010) where it is argued that in the local Universe galaxies below $\sim 10^{10.5}\,\mathrm{M_\odot}$ are environmentally quenched as satellite galaxies and galaxies above that mass are primarily quenched by internal processes (so-called "mass quenching").

While it appears that the majority of low-mass galaxies are primarily quenched as satellites, there are still open questions regarding the details of the process(es) involved. One such question is which are the dominant mechanism(s) responsible for suppressing star formation in satellite galaxies? Galaxy harassment (e.g. Moore et al. 1996), mergers (e.g. Mihos & Hernquist 1994), starvation (e.g. Kawata & Mulchaey 2008), and ram-pressure stripping (e.g. Gunn & Gott 1972) have all been invoked, however no concensus exists on their relative importance in different environments. Additionally, while all of these mechanisms are capable of quenching galaxies (either through inducing rapid star formation and thus quickly using up cold gas reserves, or the stripping of gas), not all would have a strong effect on galaxy morphology. Recently, starvation and/or ram-pressure stripping are often favoured as satellite quenching mechanisms (Muzzin et al. 2014; Peng et al. 2015; Fillingham et al. 2015; Weisz et al. 2015; Wetzel et al. 2015) but it is not clear that either would strongly impact morphology, therefore in order to explain the observed correlation between galaxy star formation and morphology it seems that an additional process to efficiently drive morphological transformations is perhaps required (e.g. Christlein & Zabludoff 2004).

Also of importance is determining what are the characteristic haloes where most satellite galaxies are quenched and experience morphological transformations. Specifically, whether galaxies remain actively forming stars with late-type morphologies until passing the virial radius of high-mass clusters, or alternatively if galaxies are transformed in smaller groups prior to or during cluster infall (known as "pre-processing") (e.g. Fujita 2004). Pre-processing is often invoked to explain observational results such as passive and red fractions at large cluster-centric radii which are enhanced significantly relative to the field (Lu et al. 2012; Wetzel et al. 2012; Bahé et al. 2013; Haines et al. 2015; Just et al. 2015), as well as the prevalence of S0 galaxies in large clusters (Kodama & Smail 2001; Helsdon & Ponman 2003; Moran et al. 2007; Wilman et al. 2009). Studies have also found evidence for pre-processing by measuring the fraction of galaxies which are part of a group subhalo during infall onto a cluster, both using simulations (McGee et al. 2009; De Lucia et al. 2012; Bahé et al. 2013) and observations (Dressler et al. 2013; Hou et al. 2014).

This pre-processing and recent infall of galaxies can often imprint itself on the dynamical profile of a group or cluster. For a dynamically relaxed group it is expected that the projected velocity profile of member galaxies will resemble a Gaussian distribution. Whereas groups which are dynamically young and unrelaxed tend to display velocity profiles which are less Gaussian in nature. The degree to which galaxy properties correlate with the dynamical state of their host groups is still an open question (e.g. Biviano

et al. 2002; Ribeiro et al. 2013b). Previous work has suggested that galaxies in relaxed groups tend to be redder than galaxies in unrelaxed groups (Ribeiro et al. 2010; Carollo et al. 2013; Ribeiro et al. 2013a). However less work has been done studying the dynamical dependences of star-formation and morphology directly. One example is the work of Hou et al. (2013) who find no detectable difference between the quiescent fractions of galaxies in Gaussian versus non-Gaussian groups as a function of redshift.

Previously we have shown that the star formation and morphology of low-mass galaxies depends not only on stellar and halo mass but also on the X-ray luminosity of the host group (Roberts et al. 2016). Here we investigate the dependence of star-forming and morphological properties of galaxies on group dynamical state. In particular, we study these properties within different phase space regions of the halo to elucidate whether any dependences on dynamical state are in place during infall or whether they are not set in place until galaxies move within the virialized region.

The outline of this paper is as follows. In Section 2 we describe sample of galaxies in groups as well as our field sample. In Section 3 we outline our method of distinguishing between infalling and virialized galaxies. In Section 4 we analyze the dependence of galaxy star formation and morphology on dynamics for infalling galaxies. In Section 5 we do the same for virialized galaxies. We discuss our results in Section 6 and summarize in Section 7.

In this paper we assume a flat Λ cold dark matter cosmology with $\Omega_\mathrm{M} = 0.3$, $\Omega_\Lambda = 0.7$, and $H_0 = 70\,\mathrm{km\,s^{-1}\,Mpc^{-1}}$.

2   DATA

2.1   Group sample

For this work we employ the group catalogue of Yang et al. (2007), which is constructed by applying the halo-based galaxy group finder from Yang et al. (2005, 2007) to the New York University Value-Added Galaxy Catalogue (NYU-VAGC; Blanton et al. 2005). The NYU-VAGC is a low redshift galaxy catalogue consisting of 693 319 galaxies derived from the Sloan Digital Sky Survey Data Release 7 (SDSS-DR7; Abazajian et al. 2009). We will briefly describe the halo-based group finding algorithm used to generate the Yang group catalogue, however for a more complete description the authors direct the reader to Yang et al. (2005) and Yang et al. (2007).

First, the centres of potential groups are identified. Galaxies are initially assigned to groups using a traditional "friends-of-friends" (FOF) algorithm (e.g. Huchra & Geller 1982) with very small linking lengths. The luminosity-weighted centres of FOF groups with at least two members are then taken as the centres of potential groups and all galaxies not yet associated with a FOF group are treated as tentative centres for potential groups. A characteristic luminosity, $L_{19.5}$, defined as the combined luminosity of all group members with $^{0.1}M_r - 5\log h \leq -19.5$, is calculated for each tentative group and an initial halo mass is assigned using an assumption for the group mass-to-light ratio, $M_H/L_{19.5}$. Utilizing this tentative group halo mass, velocity dispersions and a virial radius are calculated for each group. Next, galaxies are assigned to groups under the assumption that the

distribution of galaxies in phase space follows that of dark matter particles – the distribution of dark matter particles is assumed to follow a spherical NFW profile (Navarro et al. 1997). Using the new group memberships, group centres are recalculated and the procedure is iterated until group memberships no longer change.

We take group halo masses, M_H, from the Yang catalogue calculated using a characteristic group stellar mass, $M_{\star,\mathrm{grp}}$, and assuming that there is a one-to-one relation between $M_{\star,\mathrm{grp}}$ and M_H. Yang et al. (2007) define $M_{\star,\mathrm{grp}}$ as

$$M_{\star,\mathrm{grp}} = \frac{1}{g(L_{19.5}, L_{\mathrm{lim}})} \sum_i \frac{M_{\star,i}}{C_i} \tag{1}$$

where $M_{\star,i}$ is the stellar mass of the ith member galaxy, C_i is the completeness of the survey at the position of that galaxy, and $g(L_{19.5}, L_{\mathrm{lim}})$ is a correction factor which accounts for galaxies missed due to the magnitude limit of the survey.

The Yang catalogue contains both haloes which would be broadly classified as groups ($10^{12} \lesssim M_H \lesssim 10^{14}\,\mathrm{M_\odot}$) as well as clusters ($M_H \gtrsim 10^{14}\,\mathrm{M_\odot}$), however for brevity we will refer to all haloes as groups regardless of halo mass unless otherwise specified.

We calculate group-centric radii for all group members within the sample using the redshift of the group and the angular separation of the galaxy from the luminosity-weighted centre of the host halo. Radii are normalized by the virial radius, R_{200}, of the group using the definition given in Carlberg et al. (1997)

$$R_{200} = \frac{\sqrt{3}\sigma}{10H(z)}, \tag{2}$$

where the Hubble parameter, H(z), is defined as

$$H(z) = H_0\sqrt{\Omega_{\mathrm{M}}(1+z)^3 + \Omega_\Lambda}, \tag{3}$$

and the rest-frame velocity dispersion, σ, is calculated with the Gapper Estimator (Beers et al. 1990) and applying a redshift correction (i.e. $\sigma = \sigma_{\mathrm{obs}}/[1+z]$). We only include groups with $N_{\mathrm{members}} \geq 8$ to ensure reasonable statistics both for calculating velocity dispersions and for later classifying the dynamical states of these groups.

To study specific characteristics of galaxies within the group sample, we match various public SDSS galaxy catalogues to the group sample. We utilize galaxy stellar masses given in the NYU-VAGC, which are obtained through fits to galaxy spectra and broadband photometric measurements following the procedure of Blanton & Roweis (2007).

For our star formation indicator we use specific star formation rates ($SSFR = SFR/M_\star$) from Brinchmann et al. (2004). These SSFRs are primarily derived from emission lines, with an exception for galaxies with no clear emission lines or AGN contamination in which case SSFRs are based on the 4000 Å break. SSFRs for galaxies with S/N > 2 in Hα are determined using only the Hα line and SSFRs for galaxies with S/N > 3 in all four BPT lines are determined using a combination of emission lines.

For our morphology indicator we use a global Sérsic index taken from the single component Sérsic fits in Simard et al. (2011). We also weight all of the data by $1/V_{\mathrm{max}}$ as
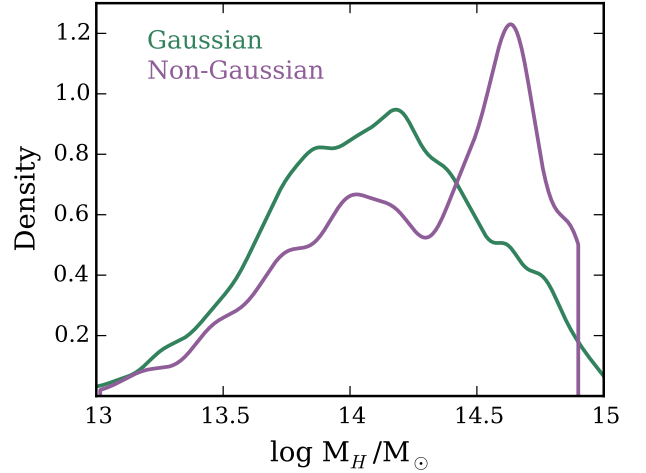

Figure 1. Smoothed host halo mass distributions for galaxies in the unmatched G and NG samples.

given in Simard et al. (2011) to account for the incompleteness of the sample.

For our analysis we consider only satellite galaxies within groups. We define central galaxies as the most-massive galaxy within a group and subsequently remove all centrals from the data set. This gives us an initial group sample of 47 961 galaxies in 2 662 groups.

2.2 Field sample

We also define a sample of "field" galaxies. Like the group sample, the field sample is also derived from the NYU-VAGC. In order to construct the field sample we cross-match galaxies within the Yang group catalogue against all galaxies within the NYU-VAGC catalogue, and remove any galaxies which have been identified as being members of Yang groups. Furthermore, we apply an isolation criteria and only keep galaxies which are separated from their nearest-neighbour by a projected distance of at least 0.5 Mpc and by at least 500 km/s in line-of-sight velocity.

Stellar masses, SSFRs, and Sérsic indices for the field sample are obtained from the same sources discussed in Section 2.1, leaving a field sample containing 65 004 galaxies.

2.3 Group dynamics

To classify the dynamical state of the haloes in the data set we use a combination of two statistical tests, the Anderson-Darling (AD) normality test (Anderson & Darling 1952; see Hou et al. 2009, 2013 for an astronomical application) and the Dip test (Hartigan & Hartigan 1985; see Ribeiro et al. 2013a for an astronomical application).

The AD test is a non-parametric test of normality based upon the comparison between the cumulative distribution function (CDF) of a measured data sample and the CDF of a gaussian distribution. Under the assumption that the data is in fact normally distributed, the AD test determines the probability (p) that the difference between the CDFs of the data and a normal distribution equals or exceeds the

observed difference. We apply the AD test to the velocity distributions of the member galaxies of each group in the data sample, thereby broadly classifying the dynamical state of each halo. All of our groups have eight or more member galaxies, and 85 per cent of our groups have five or more member galaxies within the virial radius. Our first criteria in classifying a group as Gaussian (G) is that the p-value given by the AD test be greater than or equal to 0.05.

Our second criteria required for a group to be classified as G is that it be unimodal. Ideally one would hope that standard normality tests would detect all instances of multimodality, however this is not always the case. In particular, multimodality in distributions with modes at small seperations can be missed by standard statistical techniques (Ashman et al. 1994). To gauge the modality of the velocity distribution of a given group we use the Dip test. Like the AD test, the Dip test is also a non-parametric CDF statistic. Where they differ is that the Dip test looks for a flattening of the CDF for the data which would correspond to a 'dip' in the distribution being tested. The Dip test operates under the null hypothesis that the data is unimodal, and we consider a group velocity distribution unimodal if the Dip test p-value is greater than or equal to 0.05. Therefore our G data sample consists of all those groups with $p_{ad} \geq 0.05$ *and* $p_{dip} \geq 0.05$, whereas our non-Gaussian (NG) data sample consists of all those groups with $p_{ad} < 0.05$ *or* $p_{dip} < 0.05$.

After applying the above criteria we find a G sample consisting of 42 655 galaxies within 2 447 groups and a NG sample consisting of 5 306 galaxies within 215 groups. We find that the AD test is the stronger discriminator compared to the Dip test as out of all of the galaxies making up the NG sample, 90 per cent failed the AD test but passed the Dip test, 8 per cent passed the AD test but failed the Dip test, and 2 per cent failed both the AD test and the Dip test. The authors note that it is easier to statistically identify NG groups for groups with high galaxy membership, this can lead to the NG sample being skewed toward large halo masses (see Fig. 1). To address this we match of G and NG samples by halo mass (as well as stellar mass and redshift), as described in the following section.

2.4   Matched data set

To ensure a fair comparison between galaxies in different environments (ie. field galaxies, galaxies in G groups, and galaxies in NG groups) we match our sample of G group galaxies and NG group galaxies by stellar mass, redshift, and halo mass. Additionally, we then match our sample of field galaxies by stellar mass and redshift. The matching is particularly important when trying to elucidate information on the effect of group dynamics on galaxy SF and morphological properties for two main reasons:

First, stellar mass, redshift, and halo mass have all been shown to influence galaxy SF and morphology (e.g. Brinchmann et al. 2004; Feulner et al. 2005; Zheng et al. 2007; Cucciati et al. 2012; Wetzel et al. 2012; Lackner & Gunn 2013; Tasca et al. 2014); whereas the impact of group dynamics is less clear (Hou et al. 2013; Ribeiro et al. 2013a) which is likely suggestive of a more modest role. Therefore, if one hopes to identify trends in galaxy SF and morphology with group dynamics it is crucial to properly control for these other known correlations.

Second, standard statistical normality tests, such as the AD test, are biased towards identifying non-Gaussian distributions when sample size is large. This is a result of the statistical power of the test increasing with sample size which subsequently allows the detection of more and more subtle departures from normality (Razali & Wah 2011). While these subtle departures from normality will perhaps be statistically significant, they may not be physically relevant (in principle, no group is truly Gaussian) and what really matters is whether galaxies in groups which show large departures from normality have different properties than galaxies in groups which show smaller departures from normality. Since group richness generally scales with halo mass, in the absence of any matching procedure, a sample of NG groups will be biased towards large halo masses compared to a similar sample of G groups – even though many high halo mass NG groups may have been identified on the basis of very small departures from normality. Ensuring that our G and NG samples have very similar halo mass distributions allows us to make a fairer comparison between the two samples.

Our algorithm for matching the G and NG samples is as follows:

1. Our list of galaxies found in NG groups is iterated through, for each galaxy one 'matching' galaxy from the G sample is found. To be considered matching the two galaxies must have stellar masses within 0.1 dex, redshifts within 0.01, and halo masses within 0.1 dex.

2. Step 1 is repeated until no more matches are found. The end result is a list of galaxies from the NG sample each of which will have one or more matching galaxies from the G sample assigned to them

3. The matched G sample is generated by including two galaxies from the G sample for every one matching galaxy from the NG sample. By definition this excludes any galaxies in the NG sample which only have one identified match. However, 85 per cent of galaxies in the NG sample have two or more matches so although we reduce the NG sample size by 15 per cent it allows us to increase the matched G sample size twofold. It is worth noting that when we run our analysis keeping only one matched G galaxy instead of two, we find no changes in the trends observed.

4. In the case where a given galaxy in the NG sample has more than two identified matches, the two matching galaxies from the G sample are chosen randomly. This introduces a stochastic nature to our analysis as each generation of the matched G sample will not contain exactly the same galaxies. To account for this, any quantities calculated using the matched G sample are done so in a Monte Carlo sense where the median of 1000 stochastic generations is quoted along with 90 per cent confidence intervals.

The field sample is subsequently matched to the NG sample following the same procedure and the same method is used to account for the stochastic nature of the matching procedure. Fig. 2 shows smoothed density distributions of stellar mass, redshift, and halo mass for the matched G, NG, and field samples. For the remainder of the paper all analysis is done using the matched samples, therefore from this point forward any reference to the G, NG, or field samples refers to the matched samples.
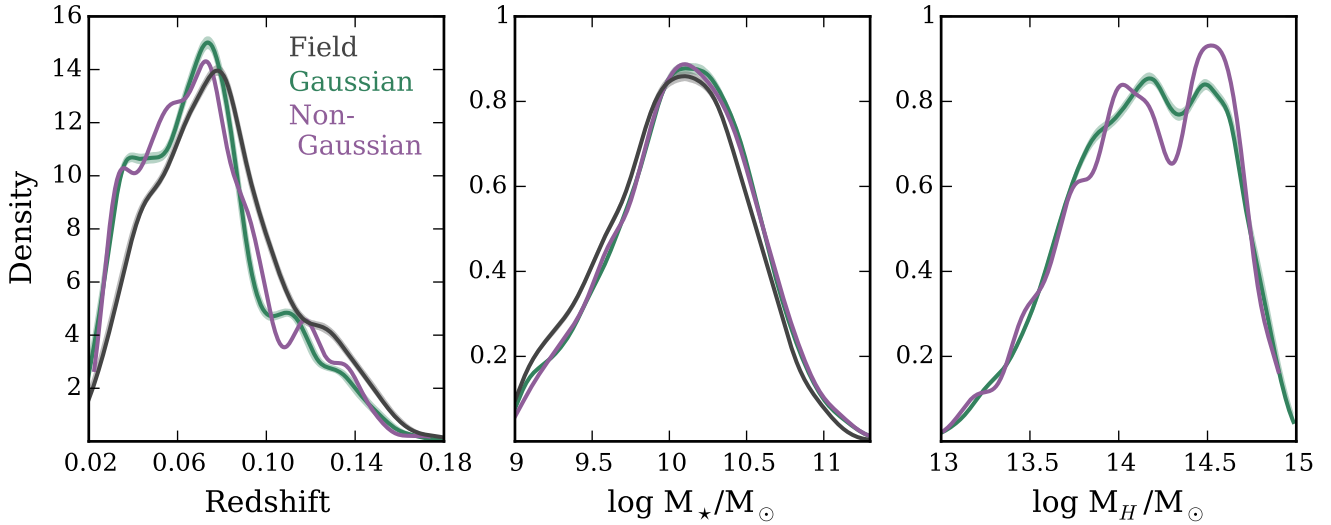
Figure 2. Smoothed distributions for stellar mass, redshift, and host halo mass for galaxies in the matched G, NG and field (where applicable) samples. Shaded regions around the G and field lines are 90 per cent confidence intervals corresponding to the stochastic nature of our matching procedure.
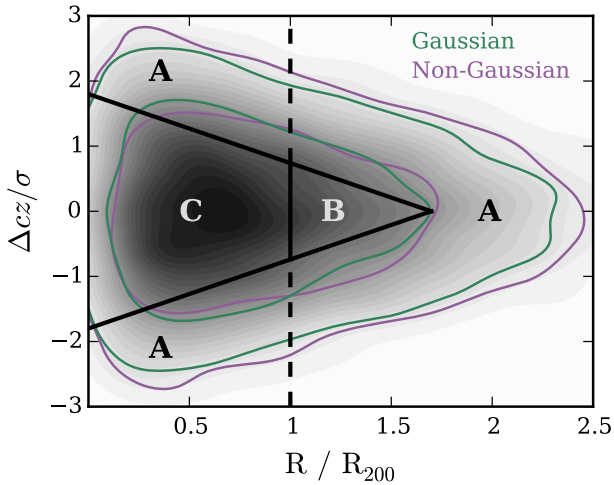

Figure 3. Projected radial phase space for galaxies within the group sample. Grey shading shows the phase space density distribution for all group galaxies, green and purple contours correspond to the 68 and 95 per cent density regions for G and NG galaxies respectively. Virialized (C), backsplash (B), and infalling (A) regions using the cuts defined in Mahajan (2011) are shown.

3 IDENTIFYING INFALLING AND VIRIALIZED GALAXIES

Galaxies within group haloes can be broadly classified into three main subclasses: galaxies infalling to the group at large radii, galaxies virialized within the inner regions of the halo, and galaxies backsplashing beyond the virial radius after making a passage through the group centre. In order to understand the radial dependence of galaxy properties within groups it is crucial to be able to identify these different galaxy populations (Gill et al. 2005; Mahajan et al. 2011; Pimbblet 2011; Haines et al. 2015; Noble et al. 2016).

One method used to distinguish between infalling, virialized, and backsplash populations is to look for distinct populations in radial phase space. In particular Mahajan et al. (2011) follow Sanchis et al. (2004) and identify galaxies within one virial radius as virialized and use the cut

$$\frac{v_r}{V_{\rm v}} = -1.8 + 1.06 \left(\frac{r}{R_{\rm v}} \right) \tag{4}$$

to distinguish between infalling and backsplash galaxies. Where v_r is the radial velocity of the galaxy, $V_{\rm v}$ is the velocity dispersion of the group, r is the group-centric radius, and $R_{\rm v}$ is the virial radius of the group.

The cuts described above were determined using full 6-d phase space information in simulations, however observationally we are limited to line-of-sight velocities and projected radii. Although working in projection removes much of the distinct phase space structure (Oman et al. 2013; Haines et al. 2015), density contours for the virialized, backsplash, and infalling populations still occupy similar regions in projected phase space with the contamination between different populations being more substantial (Mahajan et al. 2011). While the divisions between populations is certainly less clear in projection, equation 4 can still be used to obtain an approximate division between infalling, virialized, and backsplash galaxies – this approximation is preferred over the incorrect assumption that all galaxies beyond the virial radius are infalling for the first time. In particular, at intermediate radii, $1 < R < 1.5\,R_{200}$, as much as 60 per cent of the galaxy population could be backsplashing (Mahajan et al. 2011; Hou et al. 2014).

To make the transformation to observational quantities we replace $v_r/V_{\rm v}$ with $\Delta cz/\sigma$ and $r/R_{\rm v}$ with R/R_{200} in equation 4. We also symmetrize the phase space cuts to account for projection by using the mirror of equation 4. After imple-

menting these observational adjustments, and utilizing the best-fitting scheme from Mahajan et al. (2011), we show the phase space distribution of the total group sample, as well as galaxies in G and NG groups, in Fig. 3. In addition, we divide the phase space into the infalling (Regions A), backsplash (Region B), and virialized (Region C) populations.

4 GALAXY PROPERTIES IN THE INFALL REGION

We first consider the star-forming and morphological properties of galaxies infalling (Regions A in Fig. 3) onto both G and NG groups, as well as galaxies within the field sample. We apply a lower stellar mass cut at $10^{9.5}\,\mathrm{M_\odot}$ in order to avoid including galaxies with large $1/V_{\mathrm{max}}$ weights. In Fig. 4 we plot star-forming and disc fraction of infalling galaxies versus stellar mass for the three different galaxy samples. We define star-forming galaxies to be all galaxies with $\log SSFR \geq -11$, Wetzel et al. (2012) show that in the local Universe the division between the red sequence and the blue cloud is consistently found at $\log SSFR \simeq -11$ across a wide range of halo masses. Likewise we define disc galaxies to be all galaxies having a global Sérsic index of $n \leq 1.5$. While the distribution of Sérsic index is not as clearly bimodal as the SSFR distribution, we find that our observed trends are insensitive to our exact choice of dividing Sérsic index.

Inspection of Fig. 4 reveals certain interesting features. First, there is no significant difference between the starforming or disc fractions for galaxies infalling onto G groups compared to galaxies infalling onto NG groups. This suggests that any influence that the dynamical state of the group has on star forming or morphological properties is not in place during a galaxies first infall toward the virialized region of the halo. Additionally very similar trends are observed for both star-forming and disc fractions.

We also see only a small excess of star-forming galaxies in the field compared to galaxies falling into haloes. When looking at disc fraction, this "field excess" is very marginal. Previous studies (Lewis et al. 2002; Gray et al. 2004; Rines et al. 2005; Verdugo et al. 2008) have found that star formation of galaxies within infall regions remains suppressed compared to the field out to radii on the order of $2-3\,R_{200}$. This suppression is often attributed to backsplash galaxies which have already made a passage through the halo centre, the pre-processing of galaxies in small groups prior to infall, or some combination of the two. Using the cuts described in Section 4 we have attempted to "clean" our infall sample of backsplashing galaxies, although there is still some level of contamination due to the lack of full phase space information.

It is expected that pre-processing should play a more important role in large clusters compared to smaller groups, as a larger fraction of galaxies infalling onto clusters will have been a part of a group prior to infall. This is simply a result of the hierarchical build-up of structure and the fact that regions of space around large clusters are not average but are preferentially populated with other dense structures such as group haloes (e.g. Mo & White 1996; Wang et al. 2008).

We look for evidence of pre-processing by examining

the "field excess", which we define as the difference in star forming or disc fraction between field galaxies and galaxies infalling into haloes, for different halo mass ranges. Specifically, we split our group sample into three halo mass bins: $10^{13} < M_H \leq 10^{14}\,\mathrm{M_\odot}$, $10^{14} < M_H \leq 10^{14.5}\,\mathrm{M_\odot}$, and $10^{14.5} < M_H \leq 10^{15}\,\mathrm{M_\odot}$. Since we see no strong differences between infalling galaxies for G and NG groups in any of our halo mass bins, we measure field excess with respect to the star-forming and disc fractions of all infalling galaxies regardless of whether they are infalling onto a G or NG group. In Fig. 5 we show the field excess, in star-forming fraction and disc fraction, and its dependence on halo mass. We see that field excess tends to increase with halo mass, with a star-forming field excess of up to ~ 15 per cent in rich clusters. This trend is clearest when considering starforming fraction and it is less obvious when considering disc fraction – though we do still see an excess of disc galaxies compared to the field for the higher halo masses. The observed field excess is consistent with pre-processing, as the expected relatively high degree of pre-processing of galaxies falling into clusters would drive a larger deviation from the field population, and similarly the lower expected levels of pre-processing for smaller groups would lead to a smaller difference between galaxies infalling into these groups and galaxies in the field. In Fig. 5 we shade in gray a region at high stellar mass where a sharp upturn is observed, we do this to highlight that at these masses the Monte Carlo uncertainty due to the stochastic nature of our matching procedure is large compared to the statistical errors (see Fig. 4) and therefore this upturn could simply be a result of random fluctuations.

5 GALAXY PROPERTIES IN THE VIRIALIZED REGION

We now consider star-forming and disc fractions for galaxies within the virialized region of the halo (Region C in Fig. 3), and again consider the differences between the G, NG, and field samples. Fig. 6 shows star-forming and disc fractions versus stellar mass for the three galaxy samples. In contrast to the infalling region, when considering star-forming and disc fractions for galaxies within the virialized region of the halo a subtle dependence on group dynamics emerges. In particular, galaxies in G groups have the lowest star-forming and disc fractions, and galaxies in NG groups have intermediate values – larger star forming and disc fractions than galaxies in G groups but significantly smaller than galaxies in the field. Moreover, we only observe this difference between the G and NG samples for galaxies $\lesssim 10^{10}\,\mathrm{M_\odot}$, for stellar masses higher than this threshold no dependence on group dynamics is observed. As with the infalling region (Fig. 4), we see qualitatively similar trends in both star forming and disc fractions.

6 DISCUSSION

6.1 The impact of group dynamical state

The question of to what degree group dynamical state influences galaxy properties is one which has not yet been
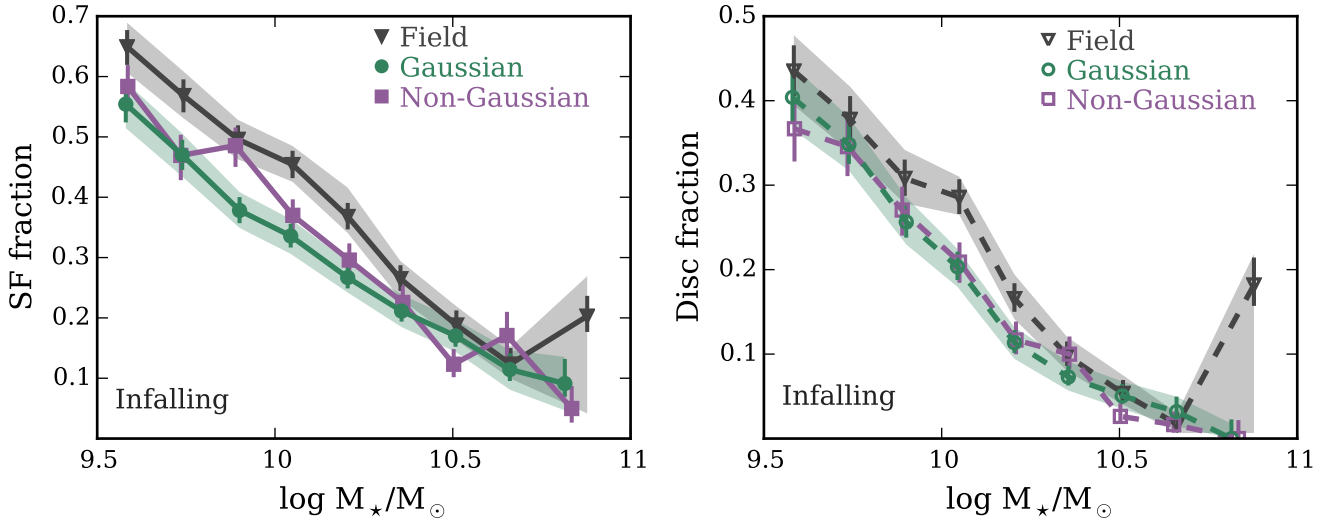
Figure 4. Star forming (left) and disc (right) fraction versus stellar mass for field galaxies as well as infalling galaxies in the G and NG samples. Error bars correspond to 1σ binomial confidence intervals as given in Cameron (2011), shaded regions are 90 per cent Monte Carlo confidence intervals derived from the stochastic nature of the matching procedure for the G and field samples.

conclusively answered. In this study we find that properties of low-mass galaxies within the inner regions of haloes show a dependence on group dynamics. In particular, we find that galaxies in the virialized region of NG groups show an increase in both star-forming and disc fractions when compared to galaxies in the same region of G groups.

Carollo et al. (2013) study the differences between galaxies in 'relaxed' and 'unrelaxed' groups (defined based upon the presence, or lack thereof, of a well defined central group galaxy) in the Zurich Environmental Study. Carollo et al. (2013) find that $< 10^{10}\,M_\odot$ satellites show slightly redder colours in relaxed groups compared to unrelaxed groups. Given the general correlations between galaxy colour, star formation, and morphology, this agrees well with the findings of this work. Ribeiro et al. (2013a) use a statistical metric designed to quantify the distance between probability density functions, known as the Hellinger distance, to discriminate between G and NG groups using a FOF catalogue of SDSS group galaxies (Berlind et al. 2006). They find no dependence on group dynamics for bright galaxies ($M_r \le -20.7$), however find that properties of faint galaxies ($-20.7 < M_r \le -17.9$) do depend on whether they live in a G or NG group. Relevant to this work, Ribeiro et al. (2013a) show that faint galaxies in G groups are redder than their NG counterparts. As well Ribeiro et al. calculate mean colours for galaxies in the inner and outer region of the halo (dividing the inner and outer halo at the median radius) for G and NG groups. They find that the colours of galaxies in NG groups do not change radially, but galaxies in the inner region of G groups are redder than those in the outer region.

The results of this paper can be used to further constrain the connection between group dynamics and the quenching of star formation as well as morphological transformations. The main result that we observe a dependence on dynamics in the virialized region of the halo but not for galaxies infalling for the first time seems to suggest quench-

ing and morphological transformations primarily take place within the virial radius, and are more efficient in G groups than NG groups. Alternatively, the observed excess of star-forming, disc galaxies in NG groups could be due to the more dynamically complex NG groups having assembled more recently, therefore galaxies in G groups will have been exposed to quenching mechanisms within the group environment for longer. Examination of Fig. 6 shows that very similar trends are observed between the virialized G and NG populations when considering either star formation or morphology.

6.2 Pre-processing of infalling galaxies

In addition to star formation quenching and morphological transformations within the current host halo, we also find evidence for pre-processing in both star formation and morphology. To probe pre-processing we measure the "field excess" (ie. the degree to which star-forming and disc fractions are enhanced in the field relative to the infalling region of groups). Assuming that any environmentally driven quenching or morphological transformations occur within the virialized region of a halo, then the field excess will just correspond to the fraction of infalling galaxies which have been pre-processed. Using this we quantitatively determine the level of pre-processing by computing the field excess for low-mass ($M_\star \lesssim 10^{10.3}\,M_\odot$) and high-mass ($M_\star \gtrsim 10^{10.3}\,M_\odot$) galaxies in our three halo mass bins. In Fig. 7 we plot the fraction of low-mass and high-mass infalling galaxies which have had star formation or morphology pre-processed. We further divide into bins of halo mass to display the halo mass dependence of pre-processing. Both star formation and morphology are pre-processed, with the fraction of pre-processed galaxies ranging between ~ 0 and ~ 15 per cent when considering star-forming fraction and ~ 0 and ~ 10 per cent when considering disc fraction, depending on stellar and halo mass. Low-mass galaxies show stronger pre-processing
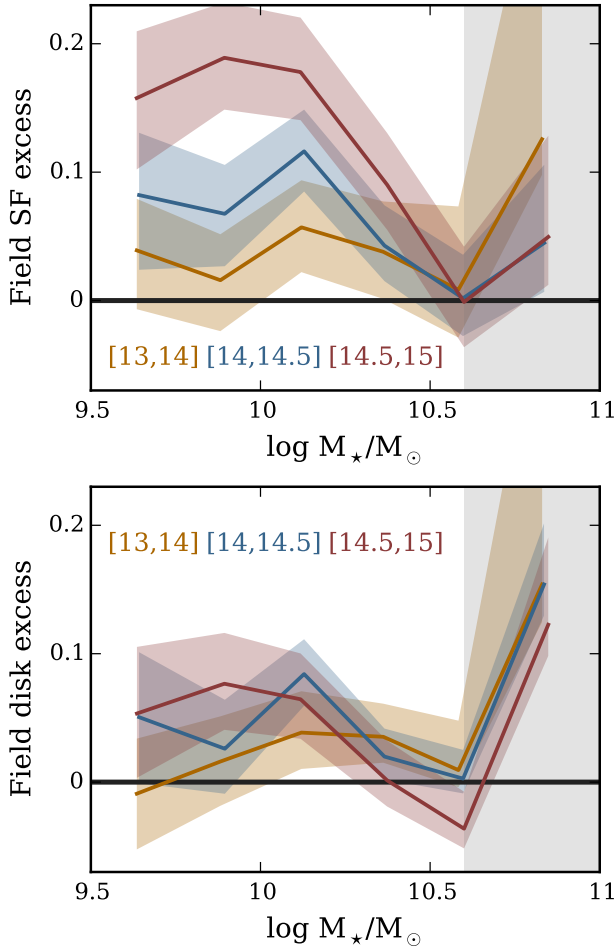
Figure 5. The excess in star-forming (top) and disc (bottom) fraction for galaxies in the field versus galaxies in the infall region of groups. We show field excess versus stellar mass for three different halo mass ranges: $10^{13} < M_H \leq 10^{14}\,\mathrm{M_\odot}$ (goldenrod), $10^{14} < M_H \leq 10^{14.5}\,\mathrm{M_\odot}$ (blue), and $10^{14.5} < M_H \leq 10^{15}\,\mathrm{M_\odot}$ (red). Shaded bands indicate 1σ statistical errors (Cameron 2011), the region at high stellar mass shaded in gray indicates where Monte Carlo errors from our matching procedure become large compared to the statistical uncertainties.

than their high-mass counterparts and the strength of pre-processing increases with halo mass.

Prior studies have aimed to constrain the fraction of pre-processed galaxies both observationally and using simulations. One common approach is to measure the fraction of galaxies which fall onto a cluster as a member of a smaller group, either directly using simulations or by measuring substructure or clustering observationally. For clusters with mass $\sim 10^{14}\,\mathrm{M_\odot}$ De Lucia et al. (2012) use semi-analytic models (SAMs) and find that the fraction of satellite galaxies which are accreted in groups with $M_H \gtrsim 10^{13}\,\mathrm{M_\odot}$ is highest for low-mass galaxies, corresponding to ~ 28 per cent. Also using SAMs, McGee et al. (2009) find that the fraction of galaxies accreted onto the ultimate cluster as members of $\gtrsim 10^{13}\,h^{-1}\,\mathrm{M_\odot}$ groups depends strongly on the cluster halo mass, ranging from ~ 0.1 for $10^{13.5}\,h^{-1}\,\mathrm{M_\odot}$ haloes to ~ 0.45 for haloes with masses of $10^{15}\,h^{-1}\,\mathrm{M_\odot}$. Bahé et al. (2013) use

the GIMIC suite of zoom in simulations and find that the fraction of galaxies which have been satellites of a $> 10^{13}\,\mathrm{M_\odot}$ halo prior to accretion onto the ultimate host ranges from < 10 per cent for a host with halo mass $< 10^{13.5}\,\mathrm{M_\odot}$, up to as high as ~ 60 per cent for a host halo mass of $10^{15.2}\,\mathrm{M_\odot}$. Observationally, Hou et al. (2014) use the Dressler-Schectman test (Dressler & Shectman 1988) to identify infalling subhaloes and find for $< 10^{14}\,\mathrm{M_\odot}$ groups that less than 5 per cent of infalling galaxies are part of a subhalo, whereas for haloes with masses $10^{14} < M_H < 10^{14.5}\,\mathrm{M_\odot}$ and $M_H > 10^{14.5}\,\mathrm{M_\odot}$ the fraction of galaxies infalling in subhaloes is ~ 10 per cent and ~ 25 per cent, respectively. Qualitatively the pre-processing trends observed in this work are consistent with these previous studies, namely the fraction of pre-processed galaxies tends to decrease with increasing galaxy stellar mass and increase with the halo mass of the host which the galaxies are infalling onto. The subhalo fraction found in these works is essentially an upper limit on the field excess quantity which we quote. This is because only some fraction of galaxies within subhaloes during infall will actually have been pre-processed, whereas the field excess more closely measures the fraction of galaxies which have actually been pre-processed. Therefore the fact that our values for the fraction of pre-processed galaxies are consistently smaller than the quoted subhalo fractions is entirely consistent.

Studying the star-forming fractions of cluster galaxies, Haines et al. (2015) use a simple toy model in an attempt to reproduce the trend between cluster-centric radius and star-forming fraction. They find that in order to reproduce the observational trend, a 19 per cent decrease in the star-forming fraction of cluster galaxies relative to the field is required on top of star formation quenching occuring within the virial radius. Haines et al. suggest that pre-processing is a possible mechanism to generate this 19 per cent decrease. In this work we find that the fraction of high-mass (the Haines et al. sample consists of galaxy stellar masses $> 2 \times 10^{10.2}\,\mathrm{M_\odot}$) pre-processed galaxies for high-mass clusters is 8 ± 3 per cent. Therefore, this work is not able to account for the amount of pre-processing required by the Haines et al. (2015) model.

At $\sim z = 0.2$, Lu et al. (2012) find that blue fractions of low and intermediate-mass cluster galaxies are lower than the field values (for the appropriate stellar mass) out to radii of $7\,\mathrm{Mpc}$, however the most massive galaxies show no difference from the field. This is similar to the stellar mass trends observed in this work where we only see strong pre-processing for low-mass galaxies.

Evidence for the pre-processing of both star formation and/or morphology is something that has been seen in recent literature, and seeing as we detect the pre-processing of both star formation and morphology in this work it is interesting to compare the level of pre-processing between the two. In general we find that the fraction of low-mass galaxies which have been morphologically pre-processed is slightly smaller than the fraction of low-mass galaxies which have had their star formation pre-processed, this is consisent across our different halo mass bins.
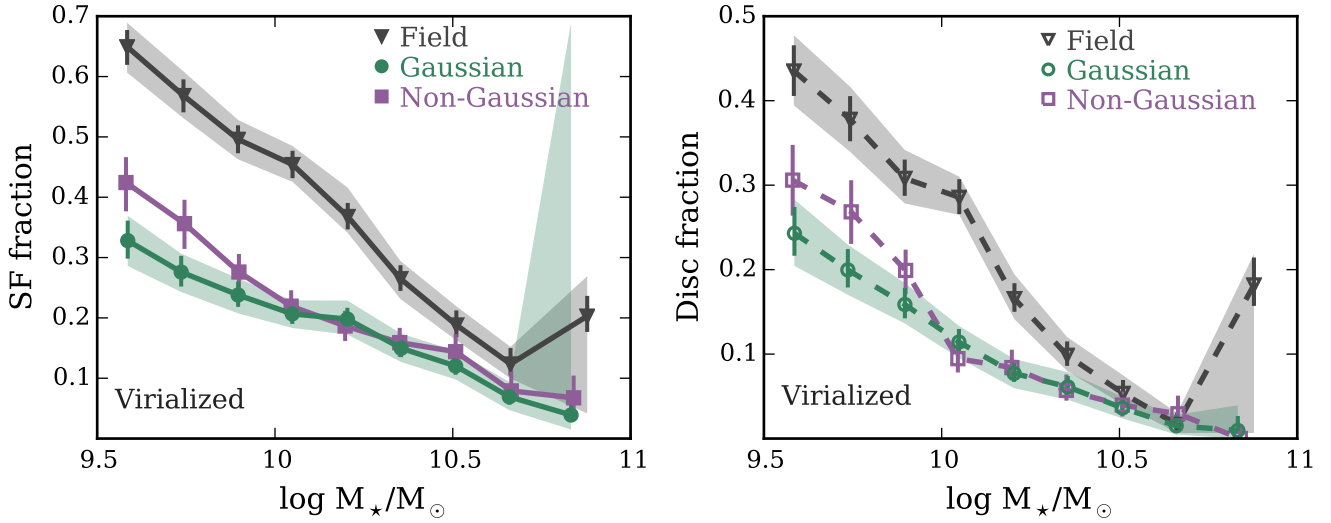
Figure 6. Star-forming (left) and disc (right) fraction versus stellar mass for field galaxies as well as virialized galaxies in the G and NG samples. Error bars correspond to 1σ binomial confidence intervals as given in Cameron (2011), shaded regions are 90 per cent Monte Carlo confidence intervals derived from the stochastic nature of the matching procedure.
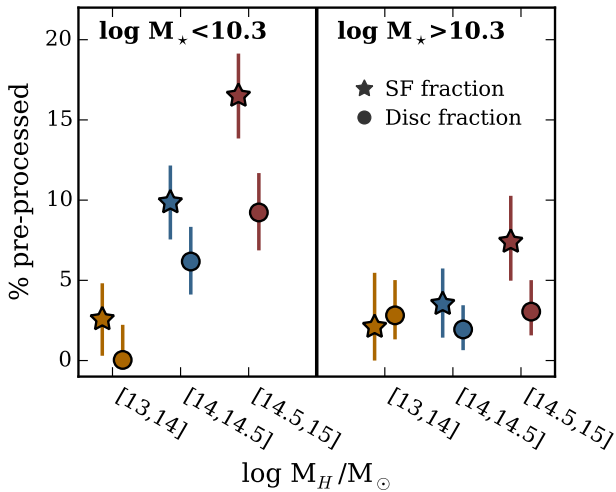

Figure 7. Pecentage of infalling galaxies which have had star-formation (stars) or morphology (circles) pre-processed for both low-mass ($M_\star \lesssim 10^{10.3}\,\mathrm{M_\odot}$, filled markers) and high-mass ($M_\star \gtrsim 10^{10.3}\,\mathrm{M_\odot}$, open markers) galaxies, as a function of halo mass. Error bars correspond to 1σ binomial confidence intervals (Cameron 2011).

7 SUMMARY & CONCLUSIONS

In this paper we investigate the dependence of galaxy properties (namely, star-forming and disc fractions) on host group dynamics. To do so we construct a carefully matched sample of galaxies housed in Gaussian groups, galaxies housed in non-Gaussian groups, as well as field galaxies; all with similar distributions in stellar mass, redshift, and (field galaxies excluded) halo mass. We then compare the properties of these different samples for two different regions within

the halo: the infalling region, and the virialized region. The main findings of this work are as follows:

1. Star-forming and disc fractions of infalling galaxies do not depend on the dynamics of the group that they are falling onto.

2. We detect pre-processing by measuring the difference between the star-forming and disc fractions for field galaxies compared to infalling galaxies. Infalling galaxies have had both star formation and morphology pre-processed, with low-mass galaxies infalling onto high-mass haloes showing the largest degree of pre-processing.

3. Galaxies in the virialized region of the halo show a clear dependence on group dynamical state. Low-mass galaxies in non-Gaussian groups show enhanced star-forming and disc fractions compared to galaxies in Gaussian groups at the same stellar mass.

the Higher Education Funding Council for England. The SDSS Web Site is http://www.sdss.org/.

REFERENCES

Abazajian K. N., et al., 2009, ApJS, 182, 543

Anderson T. W., Darling D. A., 1952, The Annals of Mathematical Statistics, 23, 193

Ashman K. M., Bird C. M., Zepf S. E., 1994, AJ, 108, 2348

Bahé Y. M., McCarthy I. G., Balogh M. L., Font A. S., 2013, MNRAS, 430, 3017

Bamford S. P., et al., 2009, MNRAS, 393, 1324

Beers T. C., Flynn K., Gebhardt K., 1990, AJ, 100, 32

Berlind A. A., et al., 2006, ApJS, 167, 1

Biviano A., Katgert P., Thomas T., Adami C., 2002, A&A, 387, 8

Blanton M. R., Roweis S., 2007, AJ, 133, 734

Blanton M. R., et al., 2005, AJ, 129, 2562

Brinchmann J., Charlot S., White S. D. M., Tremonti C., Kauffmann G., Heckman T., Brinkmann J., 2004, MNRAS, 351, 1151

Butcher H., Oemler Jr. A., 1978, ApJ, 226, 559

Cameron E., 2011, PASA, 28, 128

Carlberg R. G., et al., 1997, ApJ, 485, L13

Carollo C. M., et al., 2013, ApJ, 776, 71

Christlein D., Zabludoff A. I., 2004, ApJ, 616, 192

Cortese L., Gavazzi G., Boselli A., Franzetti P., Kennicutt R. C., O'Neil K., Sakai S., 2006, A&A, 453, 847

Cucciati O., et al., 2012, A&A, 539, A31

De Lucia G., Fontanot F., Wilman D., 2012, MNRAS, 419, 1324

Dressler A., 1980, ApJ, 236, 351

Dressler A., Shectman S. A., 1988, AJ, 95, 985

Dressler A., Smail I., Poggianti B. M., Butcher H., Couch W. J., Ellis R. S., Oemler Jr. A., 1999, ApJS, 122, 51

Dressler A., Oemler Jr. A., Poggianti B. M., Gladders M. D., Abramson L., Vulcani B., 2013, ApJ, 770, 62

Eke V. R., Baugh C. M., Cole S., Frenk C. S., King H. M., Peacock J. A., 2005, MNRAS, 362, 1233

Fasano G., et al., 2015, MNRAS, 449, 3927

Feulner G., Gabasch A., Salvato M., Drory N., Hopp U., Bender R., 2005, ApJ, 633, L9

Fillingham S. P., Cooper M. C., Wheeler C., Garrison-Kimmel S., Boylan-Kolchin M., Bullock J. S., 2015, MNRAS, 454, 2039

Fujita Y., 2004, PASJ, 56, 29

Geller M. J., Huchra J. P., 1983, ApJS, 52, 61

Gill S. P. D., Knebe A., Gibson B. K., 2005, MNRAS, 356, 1327

Goto T., Yamauchi C., Fujita Y., Okamura S., Sekiguchi M., Smail I., Bernardi M., Gomez P. L., 2003, MNRAS, 346, 601

Gray M. E., Wolf C., Meisenheimer K., Taylor A., Dye S., Borch A., Kleinheinrich M., 2004, MNRAS, 347, L73

Gunn J. E., Gott III J. R., 1972, ApJ, 176, 1

Haines C. P., La Barbera F., Mercurio A., Merluzzi P., Busarello G., 2006, ApJ, 647, L21

Haines C. P., et al., 2015, ApJ, 806, 101

Hartigan J. A., Hartigan P. M., 1985, The Annals of Statistics, 13, 70

Helsdon S. F., Ponman T. J., 2003, MNRAS, 339, L29

Hou A., Parker L. C., Harris W. E., Wilman D. J., 2009, ApJ, 702, 1199

Hou A., et al., 2013, MNRAS, 435, 1715

Hou A., Parker L. C., Harris W. E., 2014, MNRAS, 442, 406

Hubble E., Humason M. L., 1931, ApJ, 74, 43

Huchra J. P., Geller M. J., 1982, ApJ, 257, 423

Just D. W., et al., 2015, preprint, (arXiv:1506.02051)

Kawata D., Mulchaey J. S., 2008, ApJL, 672, L103

Kodama T., Smail I., 2001, MNRAS, 326, 637

Lackner C. N., Gunn J. E., 2013, MNRAS, 428, 2141

Lewis I., et al., 2002, MNRAS, 334, 673

Lu T., Gilbank D. G., McGee S. L., Balogh M. L., Gallagher S., 2012, MNRAS, 420, 126

Mahajan S., Mamon G. A., Raychaudhury S., 2011, MNRAS, 416, 2882

McGee S. L., Balogh M. L., Bower R. G., Font A. S., McCarthy I. G., 2009, MNRAS, 400, 937

McGee S. L., Balogh M. L., Wilman D. J., Bower R. G., Mulchaey J. S., Parker L. C., Oemler A., 2011, MNRAS, 413, 996

Mihos J. C., Hernquist L., 1994, ApJ, 425, L13

Mo H. J., White S. D. M., 1996, MNRAS, 282, 347

Moore B., Katz N., Lake G., Dressler A., Oemler A., 1996, Nature, 379, 613

Moran S. M., Ellis R. S., Treu T., Smith G. P., Rich R. M., Smail I., 2007, ApJ, 671, 1503

Muzzin A., et al., 2014, ApJ, 796, 65

Navarro J. F., Frenk C. S., White S. D. M., 1997, ApJ, 490, 493

Noble A. G., Webb T. M. A., Yee H. K. C., Muzzin A., Wilson G., van der Burg R. F. J., Balogh M. L., Shupe D. L., 2016, ApJ, 816, 48

Oman K. A., Hudson M. J., Behroozi P. S., 2013, MNRAS, 431, 2307

Peng Y.-j., et al., 2010, ApJ, 721, 193

Peng Y., Maiolino R., Cochrane R., 2015, Nature, 521, 192

Pimbblet K. A., 2011, MNRAS, 411, 2637

Postman M., Geller M. J., 1984, ApJ, 281, 95

Postman M., et al., 2005, ApJ, 623, 721

Rasmussen J., Mulchaey J. S., Bai L., Ponman T. J., Raychaudhury S., Dariush A., 2012, ApJ, 757, 122

Razali N. M., Wah Y. B., 2011, Journal of Statistical Modeling and Analytics, 2, 21

Ribeiro A. L. B., Lopes P. A. A., Trevisan M., 2010, MNRAS, 409, L124

Ribeiro A. L. B., de Carvalho R. R., Trevisan M., Capelato H. V., La Barbera F., Lopes P. A. A., Schilling A. C., 2013a, MNRAS, 434, 784

Ribeiro A. L. B., Lopes P. A. A., Rembold S. B., 2013b, A&A, 556, A74

Rines K., Geller M. J., Kurtz M. J., Diaferio A., 2005, AJ, 130, 1482

Roberts I. D., Parker L. C., Karunakaran A., 2016, MNRAS, 455, 3628

Sanchis T., Łokas E. L., Mamon G. A., 2004, MNRAS, 347, 1198

Schawinski K., Virani S., Simmons B., Urry C. M., Treister E., Kaviraj S., Kushkuley B., 2009, ApJL, 692, L19

Simard L., Mendel J. T., Patton D. R., Ellison S. L., McConnachie A. W., 2011, ApJS, 196, 11

Tasca L. A. M., et al., 2014, A&A, 564, L12

Verdugo M., Ziegler B. L., Gerken B., 2008, A&A, 486, 9

Wang Y., Yang X., Mo H. J., van den Bosch F. C., Weinmann S. M., Chu Y., 2008, ApJ, 687, 919

Weisz D. R., Dolphin A. E., Skillman E. D., Holtzman J., Gilbert K. M., Dalcanton J. J., Williams B. F., 2015, ApJ, 804, 136

Wetzel A. R., Tinker J. L., Conroy C., 2012, MNRAS, 424, 232

Wetzel A. R., Tollerud E. J., Weisz D. R., 2015, ApJ, 808, L27

Whitmore B. C., Gilmore D. M., Jones C., 1993, ApJ, 407, 489

Wilman D. J., et al., 2005, MNRAS, 358, 88

Wilman D. J., Oemler Jr. A., Mulchaey J. S., McGee S. L., Balogh M. L., Bower R. G., 2009, ApJ, 692, 298

Yang X., Mo H. J., van den Bosch F. C., Jing Y. P., 2005, MNRAS, 356, 1293

Yang X., Mo H. J., van den Bosch F. C., Pasquali A., Li C., Barden M., 2007, ApJ, 671, 153

Zheng X. Z., Bell E. F., Papovich C., Wolf C., Meisenheimer K., Rix H.-W., Rieke G. H., Somerville R., 2007, ApJ, 661, L41

This paper has been typeset from a TEX/LATEX file prepared by the author.